# Synthesis, anti-microbial evaluation, and *in silico* studies of novel quinoline-isoxazole hybrids

Deep P. Mandir, Shivani D. Mandir, Jignesh H. Kamdar & Satishkumar D. Tala

View supplementary material ⎆

Published online: 29 Aug 2024.

Submit your article to this journal ⎆

View related articles ⎆

View Crossmark data ⎆

Taylor & Francis
Taylor & Francis Group

Check for updates

# Synthesis, anti-microbial evaluation, and *in silico* studies of novel quinoline-isoxazole hybrids

Deep P. Mandir[a], Shivani D. Mandir[b], Jignesh H. Kamdar[c] and Satishkumar D. Tala[a] (iD)

[a]Department of Chemical Sciences, Faculty of Science, Atmiya University, Rajkot, India; [b]Department of Biotechnology, Faculty of Science, Atmiya University, Rajkot, India; [c]In-Silico Lab, Department of Microbiology, School of Science, RK University, Rajkot, India

## ABSTRACT

A series of novel quinoline-isoxazole hybrids **6a–o** has been synthesized via multistep synthetic approach involving hetero Diels-alder reaction strategy. The target compounds were obtained in good yield, using low-cost readily available starting materials using simple reaction conditions. The newly synesized compounds were confirmed using ^{1}H NMR,^{13}C NMR, and Mass spectroscopic analysis techniques. Further, compounds **6a–o** were subjected to *in vitro* antimicrobial screening against various bacterial and fungal strains, such as *Bacillus subtilis*, *Staphylococcus aureus*, *Escherichia coli*, *Salmonella typhi*, *Aspergillus niger*, and *Candida albicans*. Among these, compounds **6i**, **6j**, and **6l** were found most active having equally potent compared to standard drug Ampicillin and Gentamycin. Moreover, *in silico* studies of **6a–o** with *E. coli* DNA gyrase through molecular docking and MD simulations showed excellent binding properties of these derivatives with protein site.

## GRAPHICAL ABSTRACT
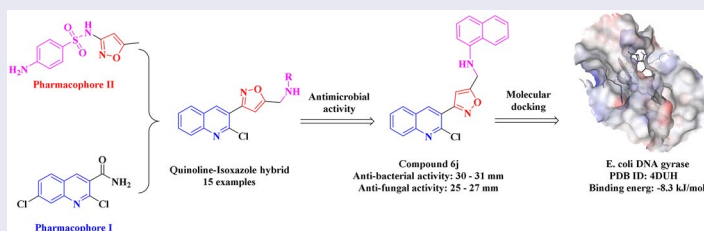


## Introduction

The majority of hospital-acquired infections are bacterial, posing a serious global health threat, increasing mortality, and straining healthcare systems worldwide.[1] One of the current threats to therapeutics is based on combating the development of anti-microbial resistance (AMR) to conventional antibiotics.[2] This bacterial resistance is such a

stubborn issue, that traditional medicine has failed to address the management of infectious diseases globally.[3] AMR is thought to have contributed to 4.95 million fatalities around the world and in expansion to straightforwardly causing 1.27 million passings.[3] The WHO alerts us to the possibility of a post-antibiotic period in the twenty-first century, in which common ailments and small mishaps could turn deadly.[4] Therefore, an alarming need to address the multidrug resistance (MDR)[5] in the bacterial strains is generated and long-term, concrete therapeutic options against potent *gram-positive* and *gram-negative* pathogens are to be created via novel and effective drugs.[6,7] The critical aspect is to design the mode of action of antibiotics in such a way that they cannot be salvaged via their metabolic and defense pathways.[8]

There are a large number of readily available medications that contain quinoline heterocycle in their structures are a good illustration of how crucial quinoline and its derivatives are in creating innovative drug moieties for therapeutic uses.[9] Quinoline is regarded as a significant biological active moiety with a wide range of biological properties, including anti-bacterial,[10] anti-oxidant,[10] anti-inflammatory,[11] anti-arrhythmic,[12] anti-convulsant,[13] anti-depressant,[14] anti-psychotic,[14] anti-hypertensive,[15,16] anti-tuberculosis,[17] anti-fungal and anti-viral[18] activities. Quinoline and its derivatives are part of several medical compounds, which include moxifloxacin (**1**, antibacterial), grepafloxacin (**2**, antibacterial), enoxacin (**3**, antibacterial), mefloquine (**4**, anti-inflammatory), chloroquine (**5**, antimalarial), ciprofloxacin (**6**, antituberculosis), and nedocromil (**7**, anticonvulsant) (Fig. 1).

On the other hand, it is widely known that isoxazole is linked to a variety of biological activities as a result of the variety of non-bonding interactions it can engage in. Numerous natural products[19] and functional materials contain the biologically active isoxazole,[20] which has a wide range of biological applications.[21] In biological systems, the isoxazole entities could easily connect with several enzymes and receptors, as evidenced by the wide range of biological functions they possess[22] including anti-bacterial,[23] anti-fungal,[24] anti-viral,[25] anti-tubercular,[26] anti-cancer,[27] and anti-inflammatory[28] activities. In addition, isoxazole and its derivatives are also found in several drug molecules like cloxacillin (**8**, antibacterial), NVP-AUY922 (**9**, anticancer), valdecoxib (**10**, anti-inflammatory), sulfamethoxazole (**11**, antibacterial) and leflunamide (**12**, anti-inflammatory).[21]

In the previous reports bioactive, and selective quinoline-isoxazole hybrids heterocycles were created[29,30] and tested for their *in vitro* cytotoxic activity against various cancer molecular targets, such as tyrosine kinase EGFR inhibition (**13**),[31] breast cancer (**14**, MCF-7),[32] melanoma murine (**15**)[33] (Fig. 1). Keeping this in mind and to continue our search for new antimicrobial agents,[34,35] we have designed and developed new quinoline-containing isoxazole derivatives (**6a–o**) and anticipated that these new hybrid derivatives may demonstrate potent activity.

## Result and discussion

### *Chemistry*

The synthetic route of quinoline containing isoxazole hybrid molecules (**6a–o**) is depicted in Scheme 1. The synthesis commenced from acetanilide (**1**) which was converted into
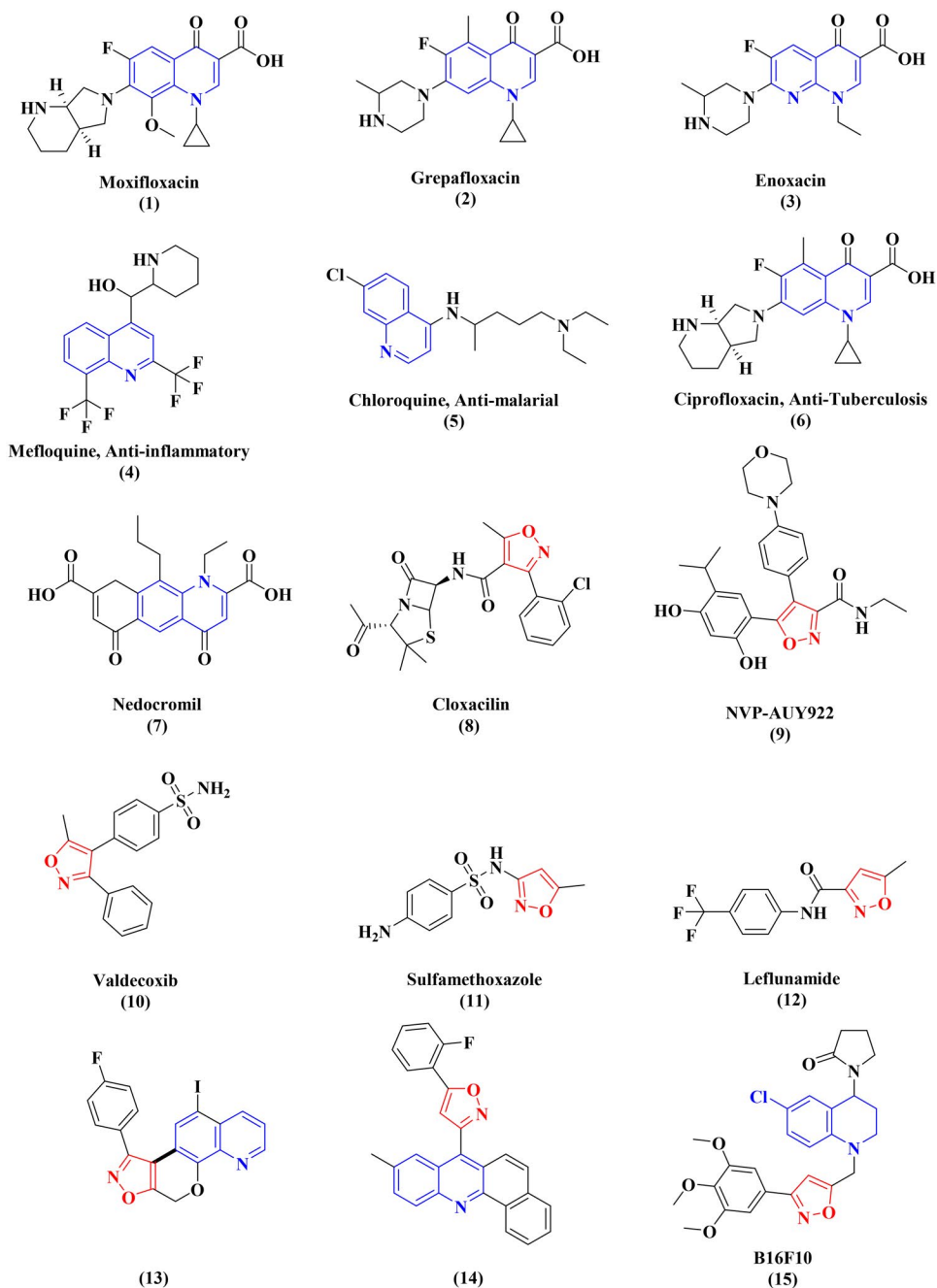
**Figure 1.** Structures of marketed drugs and active compounds having quinoline and isoxazole moieties.

the necessary intermediate 2-chloroquinoline-3-carbaldehyde (**2**) by reacting it with Vilsmeier-Haack reagent made from DMF and POCl₃ at 80 °C by the procedure outlined in the literature.[36] The required intermediate quinoline aldoxime (**3**) was produced from intermediate **2** by reacting it with hydroxylamine hydrochloride, in the presence of
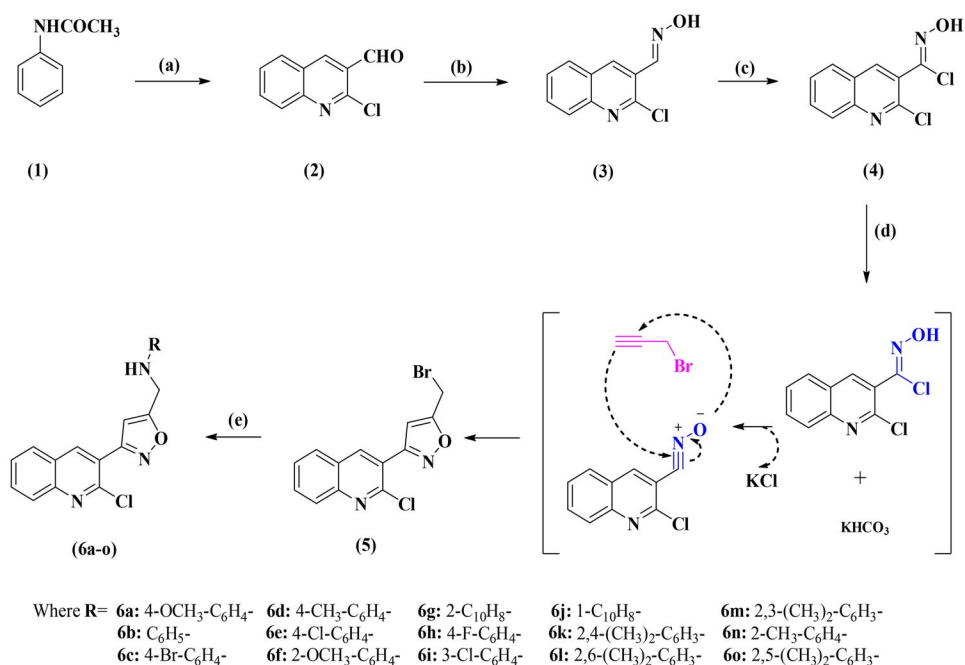
**Scheme 1.** Synthesis of the quinoline containing isoxazole derivatives. Reaction condition: (a) DMF, POCl$_3$, 80 °C, 24 h; (b) NH$_2$OH.HCl, Na$_2$CO$_3$, MeOH:Water (2:1), rt, 1 h; (c) NCS, DMF, rt, 12 h; (d) Propargyl bromide. KHCO$_3$, DMF, rt; (e) R-NH$_2$, NaHCO$_3$, THF:H$_2$O (1:1), 60 °C, 4 h.

Na$_2$CO$_3$, at room temperature by following the procedure from the literature.[37] To produce (Z)-2-chloro-N-hydroxyquinoline-3-carbimidoyl chloride (**4**), quinoline aldoxime (**3**) was reacted with N-chlorosuccinimide (NCS) in DMF at 0 °C before being allowed to attain room temperature.[38] Further, by using the hetero Diels-Alder approach, a solution of (Z)-2-chloro-N-hydroxyquinoline-3-carbimidoyl chloride (**4**) and KHCO$_3$ in DMF was treated with propargyl bromide at room temperature to produce intermediate (**5**).[39] At last, compound **5** was treated with NaHCO$_3$ and substituted aniline using THF:H$_2$O (1:1) as a solvent at 60 °C to yield the quinoline containing isoxazole derivatives (**6a–o**).[38] By examining their spectroscopic data, such as $^1$H-NMR, $^{13}$C-NMR, and mass spectroscopy, the compounds **6a–o** were characterized. For instance, the $^1$H spectrum of compound **6a** presented that 4-methoxy (OCH$_3$) protons were detected at 3.64 δppm as a singlet, and aliphatic methyl was detected at 4.52 δppm as a singlet. The aromatic region of quinoline ring protons was detected between 8.80 and 7.74 δppm and the isoxazole proton appeared as a singlet at 6.89 δppm. Substituted aniline doublet peaks were detected between 6.75 and 6.67 δppm. At 5.99 δppm a singlet peak was detected of amine (NH). A position of amine singlet peak was confirmed by D$_2$O. A representative graphical illustration of $^1$H NMR is shown in Figure 2.

## Biological activity

All the newly synthesized hybrid quinoline derivatives containing substituted isoxazole (**6a–o**) were tested for their potential activity against various gram positive [*Bacillus*
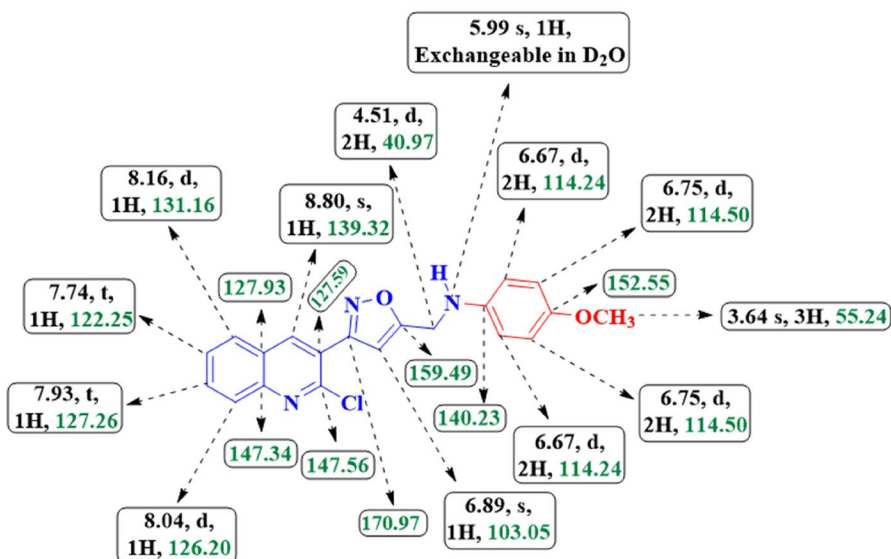
**Figure 2.** Graphical illustration of $^1$H NMR (black) and $^{13}$C NMR (green) data of representative compound **6a**.

*subtilis* (ATCC 6051 and *Staphylococcus aureus* (ATCC 23235)], gram negative [*Escherichia coli* (ATCC 25922) and *Salmonella typhi* (ATCC 19430)] and fungal strains [*Aspergillus niger* (ATCC 16888) and *Candida albicans* (ATCC 10231)]. The inhibition zone (mm) was tested against ampicillin and gentamycin as a positive control for antibacterial activity and nystatin as a positive control for antifungal activity.

As shown in Figures 3 and 4, the antimicrobial evaluation revealed that these compounds exhibited significant bioactivity against most of the tested stains with an inhibition zone ranging from 5 to 24 mm.

## Structure–activity relationship

Compound **6a** having methoxy substitution on the *para* position showed moderate to high antibacterial activity against *gram-negative* pathogens *viz. Escherichia coli* (23.6 ± 1.2 mm) and *Salmonella typhi* (25.9 ± 0.63 mm), while standard Gentamicin showed 20.8 ± 0.68 mm and 17.8 ± 0.33 mm against the respective pathogens. The phenyl ring attachment in compound **6b** (20.4 ± 0.63 mm) and compound **6c** (21.8 ± 0.63 mm) having the presence of halogen group (Br) showed a decrease in activity against *Salmonella typhi*, compared to compound **6a**. The inclusion of the electron donating group (CH$_3$) lies on the *para* position in compound **6d** (24 mm) showed good antimicrobial activity. The inclusion of the electron-withdrawing group (Cl) on the *para* position in compound **6e** (23 mm) showed good antibacterial activity against both *gram-negative* pathogens. Compound **6f** having methoxy substitution on *ortho* position showed the least inhibition in antimicrobial activity. A β-naphthyl ring system in compound **6g** showed moderate anti-bacterial activity
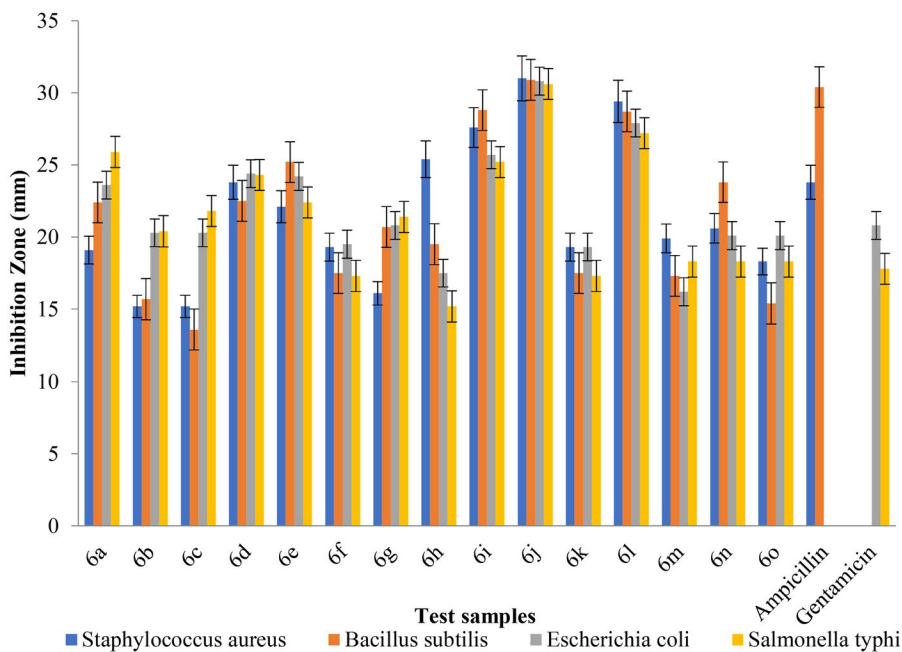
**Figure 3.** Graphical presentation of anti-bacterial activity data of newly synthesized quinoline containing isoxazole derivatives **6a–o**.

against *gram-negative* pathogens and also increased antifungal activity (20.5 mm). In compound **6h** and **6i** both have electron withdrawing groups fluro and chloro, respectively on the *para* and *meta* position. Out of which derivative **6h** showed good antibacterial activity against *gram-positive* pathogens having a zone of inhibition against *S. aureus* of $25.4 \pm 0.58$ mm and $19.5 \pm 0.58$ mm against *B. subtilis*. While derivative **6i** showed an increase in both anti-bacterial and anti-fungal activity. Compound **6j** having α-naphthyl as a substitution exhibited excellent efficacy against all the pathogens. In derivative **6k** having two methyl substitutions lies on the *ortho* and *para* position which showed moderate activity against fungal species *Candida albicans* with a zone of inhibition of $22.4 \pm 0.58$ mm. Compound **6l** also had two methyl substitutions on the *ortho* and *ortho* (*2,6*) position which exhibited very promising efficacy against all the pathogens, having a zone of inhibition (26 mm), quite greater than that of standards. Compound **6m** having the presence of two methyl substitutions on the *ortho* and *meta* position displayed the least antifungal activity but showed moderate activity against *Salmonella typhi* gram-negative pathogen with ($18.3 \pm 2.1$ mm) zone. Compounds **6n** and **6o** having methyl substitutions on the *ortho*, *ortho*, and *meta*, respectively, exhibited moderate activity against *Salmonella typhi* ($18.3 \pm 0.58$ mm and $18.3 \pm 1.2$ mm), respectively when compared with Gentamicin ($17.8 \pm 0.33$ mm). The synthesized set of compounds exhibited moderate to higher *in-vitro* anti-microbial activity and significant activity was noted in **6j** and **6l**.
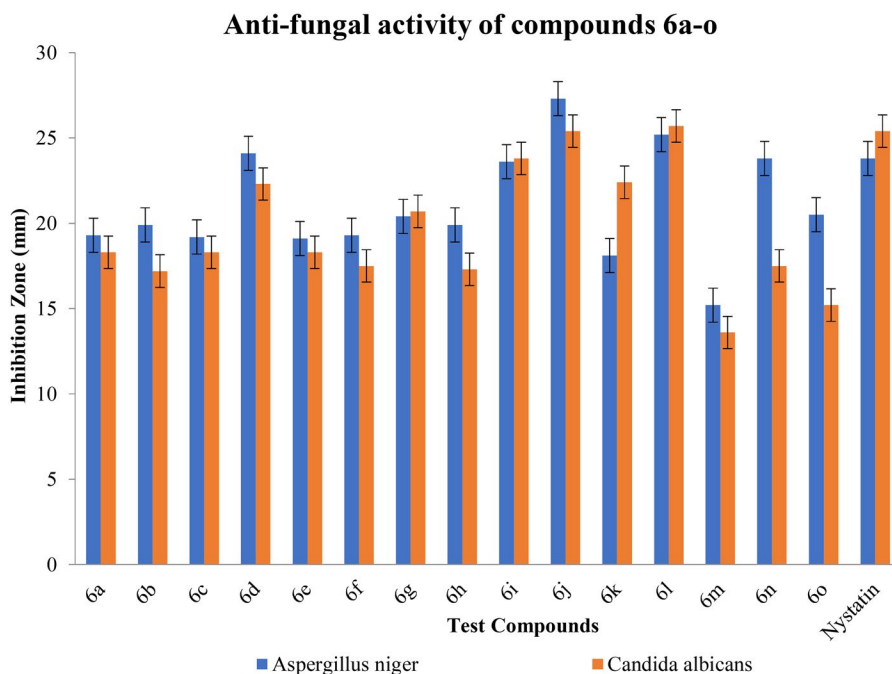
**Figure 4.** Graphical presentation of anti-fungal activity data of newly synthesized quinoline containing isoxazole derivatives **6a–o**.

## Molecular docking

*In silico* studies, especially molecular modeling an important technique for the identification of the putative binding mode of the compounds with the target protein. Hence, a molecular docking study using AutoDock Vina was carried out on the crystal structure of the crystal structure of the 24 kDa domain of *E. coli* DNA gyrase as a target for docking studies is driven by its biological significance, its potential as a drug target, the availability of structural data, and the utility of computational methods in drug discovery efforts.[40] After the energy minimization, the generated three-dimensional molecular structures were subjected to docking investigations within the binding pocket of DNA gyrase The docking study results of synthesized hybrids **6a–o** are summarized in Table 1. As evident, many amino acid residues were found in the interaction of ligands including Arg A:20, Glu B:58, Lys B:162, Asp A:17, and Arg B:204. Further, all prepared molecules exhibited good binding energy with the target varying from −7.0 to −8.3 kJmol⁻¹. Especially compound **6j** exhibited the highest docking score of −8.3 kJmol⁻¹ having two conventional hydrogen bonds with Asp A:17, and Lys B:162.

The docking studies portrayed that for compound **6a** isoxazole's nitrogen atom formed H-bonding with Arg A:20, and its –NH formed H-bindings with Glu B:58. While in the case of compound **6b** H-bonding formed with Lys B:162. In the case of compound **6c,** the halogen atom formed H-bond with Glu B:58. Compound **6d** has the same symmetrical bonding as compound **6a** oxazole's nitrogen atom, and its –NH formed two H-bonding with Arg A:20 and Glu B:58. In compound **6e** the nitrogen atom of

**Table 1.** *In silico* docking results of the newly synthesized quinoline containing isoxazole compounds **6a–o** and gentamicin with the binding site of DNA gyrase.

| Compounds | Docking score (kJ mol⁻¹) | Interacting residues | Number of H-bonds |
|---|---|---|---|
| **6a** | −7.6 | Arg A:20, Glu B:58 | 2 |
| **6b** | −7.0 | Lys B:162 | 1 |
| **6c** | −7.6 | Glu B:58 | 1 |
| **6d** | −7.7 | Arg A:20, Glu B:58 | 2 |
| **6e** | −7.6 | Lys B:162, Glu B:58 | 2 |
| **6f** | −7.2 | Asp A:17, Lys B:162 | 2 |
| **6g** | −7.8 | Lys B:162, Glu B:58 | 2 |
| **6h** | −7.6 | Lys B:162, Glu B:58 | 2 |
| **6i** | −7.7 | Asp A:17, Lys B:162 | 2 |
| **6j** | −8.3 | Asp A:17, Lys B:162 | 2 |
| **6k** | −7.5 | Arg A:20 | 1 |
| **6l** | −7.9 | Lys B:162 | 1 |
| **6m** | −7.8 | Arg A:20, Glu B:58 | 2 |
| **6n** | −7.4 | Arg B:204 | 1 |
| **6o** | −7.6 | Arg A:20 | 1 |
| Gentamicin | −6.9 | Glu A:174, Arg A:20 | 2 |
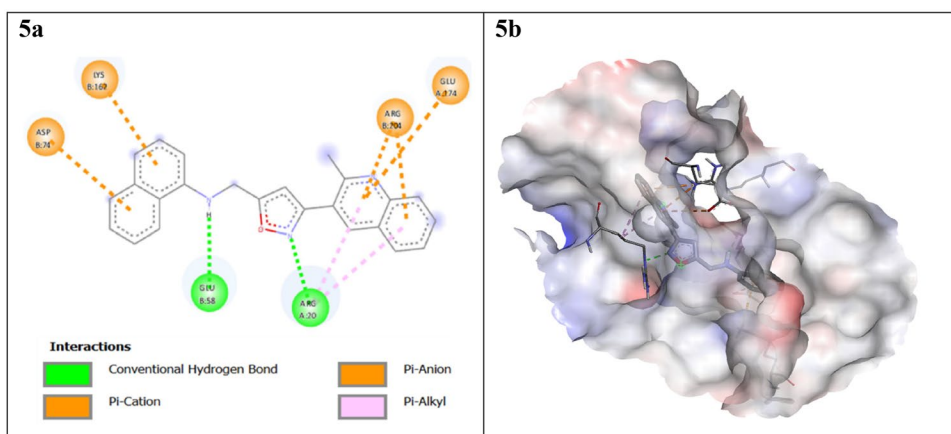


**Figure 5.** Docking pose of compound **6j** with 24 kDa domain of *E. coli* DNA gyrase. (a) Receptor-ligand interaction on a 2-D diagram, (b) receptor-ligand interaction on a 3-D diagram.

quinoline and –NH generated two H-bonding, respectively with Lys B:162 and Glu B:58. Compound **6f** formed two conventional hydrogen bonds with Asp A:17 and Lys B:162. Both compounds **6g** and **6h** showed two H-bonding with Lys B:162 and Glu B:58, out of which compound **6g** has a good docking score of −7.8 kJ mol⁻¹ as mentioned in (Table 1). Compound **6i** formed two conventional hydrogen bonds with Asp A:17 and Lys B:162. Compound **6j** also interacted with two strong H-bonding with Asp A:17 and Lys B:162, as displayed in Figure 5, with the highest docking score of −8.3 kJ/mol, shown in (Table 1). Compound **6k** made a single hydrogen bond with Arg A:20. Also, compound **6l** made a single hydrogen bond with Lys B:162, with a good docking score of −7.9 kJ mol⁻¹, as mentioned in (Table 1). Compound **6m** has two conventional hydrogen bonds with Arg A:20 and Glu B:58, with a docking score of −7.8 kJ mol⁻¹, as mentioned in (Table 1). Further, compounds **6n** and **6o** formed single H-bonding with Arg B:204 and Arg A:20, respectively. The study of reference molecule
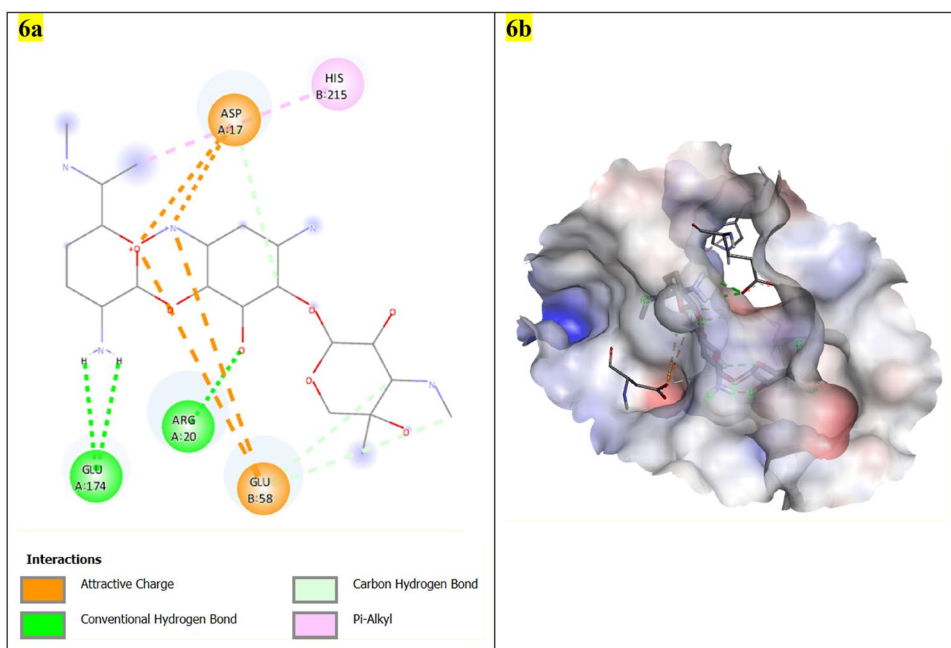
**Figure 6.** Docking pose of gentamicin with 24 kDa domain of *E. coli* DNA gyrase. (a) Receptor-ligand interaction on a 2-D diagram, (b) receptor-ligand interaction on a 3-D diagram.

gentamicin revealed that it interacted with two strong H-bonding with Arg A:20 and Glu A:174 (Fig. 6) with the lowest docking score $-6.6$ kJ mol$^{-1}$ shown in (Table 1).

## Molecular dynamics simulation analysis

The molecular dynamics technique is used to investigate the stability and conformational changes of the molecules in the simulated protein.[41] In the current work, the 24 kDa domain of *E. coli* DNA gyrase with the most potent compound **6j** was chosen for molecular dynamics modeling. The stability of the complexes was assessed using potential energy throughout a 100-ns simulation time with a 2-ns time interval. This study examined the relationships between Root Mean Square Deviation (RMSD) and Root Mean Square Fluctuations (RMSF).

## Root mean square deviation

RMSD is a measure of how far atoms move from one frame to another. The structural conformation of the protein and the stability of the ligand regarding the protein and its binding site can be inferred from the monitoring of their RMSDs, whereas the stability of the ligand can be revealed from the monitoring of the protein. Changes of 1–3 Å are acceptable for small and globular proteins. Compound **6j** and protein achieved stability with slight fluctuations during the first 12 ns of MD simulation (Fig. 7). After that, it stayed linked to the protein for the remainder of the simulation session. Furthermore, the difference in RMSD values between compound **6j** and protein
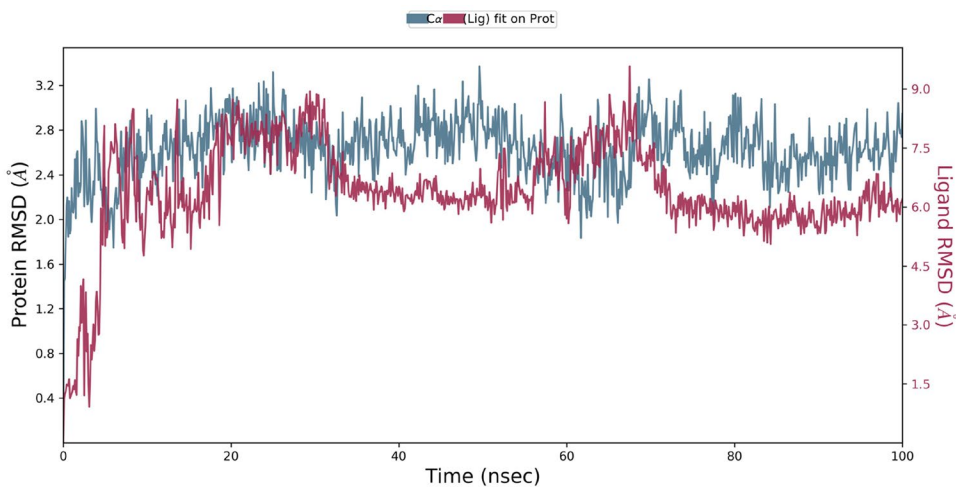
**Figure 7.** Root mean square deviation (RMSD) plot of compound **6j-protein** complex.
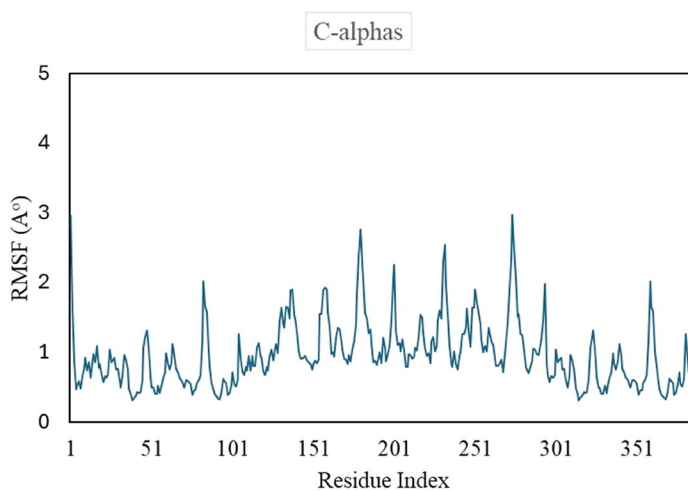


**Figure 8.** Root mean square fluctuations (RMSF) plot of compound **6j-protein** complex.

average value was 1.3 Å, which demonstrates that the **6j**-protein complex (Crystal structure of the 24 kDa domain of *E. coli* DNA gyrase, PDB ID: 4DUH) is stable.

## *Root mean square fluctuations*

The root mean square fluctuations (RMSF) show the fluctuations of each protein amino acid residue across the simulation time period. Lower RMSF values for compounds **6j** (Fig. 8) in the system imply minor structural reorganizations and conformational changes at the binding site residues during the course of the simulation. The study indicated that the structure and organization of the protein do not deviate significantly from their original conformation after interacting with the compound.
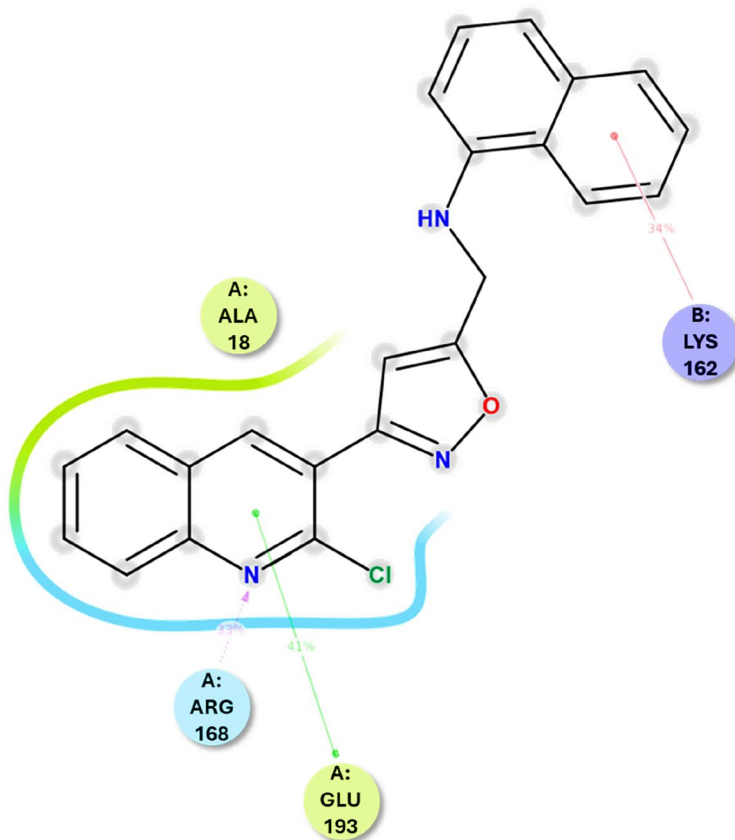
**Figure 9.** Interaction diagram of compound **6j**-protein contacts.

The ligand-protein contacts show the specific residues of the protein that interact with the ligand (Fig. 9). The ALA 18 forms several contacts with the ligand, suggesting its significant role in ligand binding. Whereas ARG 168 forms hydrogen bonds or ionic interactions with the ligand, indicated by the dashed lines connecting the nitrogen atom of ARG 168 to the ligand. The GLU 193 also forms an interaction with the ligand, likely contributing to the overall binding affinity. The protein-ligand contacts in the bar chart represent the interaction frequency of different residues with the ligand over an MDS (Fig. 10). The different colors in the bars likely represent different types of interactions, such as hydrogen bonds, hydrophobic interactions, or electrostatic interactions. Overall, the varying interaction fractions suggest that certain residues like ARG 168 are consistently involved in ligand binding, while others may have more transient interactions.

## Experimental

### *Chemistry*

This includes general procedure for the synthesis of compounds **2–6**. Experimental procedures for the intermediate and spectral data of all compounds are presented in supporting information.
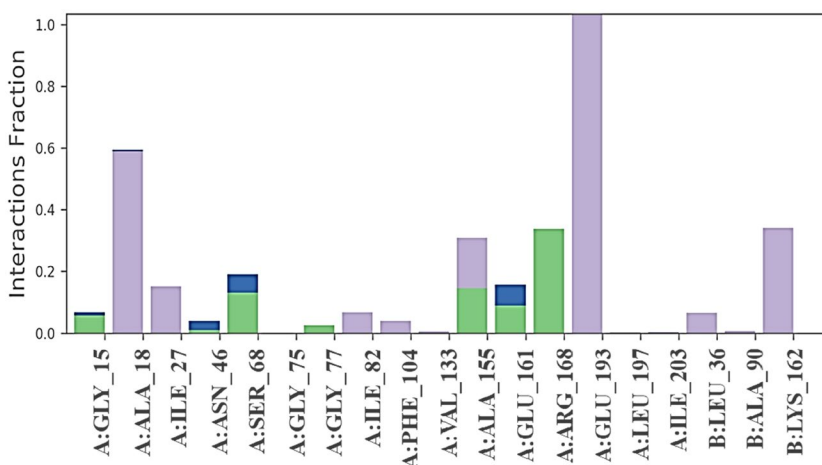
**Figure 10.** Interaction graph of protein-**6j** contacts.

## General procedure for the synthesis of compounds (6a–o)

To a well-stirred mixture of 5-(bromomethyl)-3-(2-chloroquinolin-3-yl)isoxazole (**5**, 0.80 mmol) and different substituted aniline (0.80 mmol) in a $H_2O$:THF (1:1, 12 mL), $NaHCO_3$ (0.96 mmol) was added in portions and the mixture was stirred at 60 °C for 4 h. After completion of the reaction (monitored by TLC), the reaction mixture was then poured onto crushed ice. The precipitate thus appeared was collected by filtration with suction and washed with water, and dried. The obtained residue was purified to give title compounds (**6a–o**), which are analytically pure.

## N-((3-(2-chloroquinolin-3-yl)isoxazol-5-yl)methyl)-4-methoxyaniline (6a)

By using the general synthetic procedure, compound **6a** was prepared from compound **5** (0.20 g, 0.62 mmol) and p-methoxy aniline (0.08 g, 0.62 mmol) in $H_2O$: THF (1:1, 12 mL), $NaHCO_3$ (0.06 g, 0.74 mmol).

An off-white solid (0.19 g, 94% yield); mp: 90–92 °C. IR (KBr) $v_{max}$/cm$^{-1}$: 3367 (NH), 2989 (Ar-C-H), 1606 (Ar-CH=CH), 1513 (Aromatic ring), 1328 (C-N), 1237 (C-O), 779 (C-Cl), 752 (C-OCH$_3$ Mono Substitution) cm$^{-1}$. $^1$H NMR (400 MHz, DMSO-$d_6$) δppm: 8.80 (s, 1H, Ar-H), 8.16 (d, $J$ = 7.9 Hz, 1H, Ar-H), 8.04 (d, $J$ = 8.4 Hz, 1H, Ar-H), 7.93 (t, $J$ = 7.7 Hz, 1H, Ar-H), 7.74 (t, $J$ = 7.5 Hz, 1H, Ar-H), 6.89 (s, 1H, Ar-H), 6.75 (d, $J$ = 8.3 Hz, 2H, 2 × Ar-H), 6.67 (d, $J$ = 8.6 Hz, 2H, 2 × Ar-H), 5.99 (s, 1H, NH, exchangeable in $D_2O$), 4.51 (d, $J$ = 6.4 Hz, 2H, CH$_2$), 3.64 (s, 3H, OCH$_3$); $^{13}$C NMR (101 MHz, DMSO-$d_6$) δppm: 170.97, 159.49, 152.55, 147.56, 147.34, 140.23, 139.32, 131.16, 127.93, 127.59, 127.26, 126.20, 122.25, 114.50, 114.24, 103.05, 55.24, 40.97; MS $m/z$ (%): 366 (M$^+$); Anal. Calcd. $C_{20}H_{16}ClN_3O_2$ (365.82): C, 65.67; H, 4.41; N, 11.49%. Found C, 65.71; H, 4.39; N, 11.55%.

## Protocol of antimicrobial activity

The antibacterial and anti-fungal activity was checked against the common fungal pathogens *Aspergillus niger*, and *Candida albicans*, along with the bacterial strains of

two gram-positive bacteria (*Bacillus subtilis*, *Staphylococcus aureus*) and, two gram-negative bacteria (*Escherichia coli* and *Salmonella typhi*). The antibacterial and antifungal standards Ampicillin (100 μg/ml), Gentamicin (100 μg/ml), and Nystatin (100 μg/ml), respectively were used to test the inhibition zone (mm). According to the experimental results, all bacterial strains were significantly inhibited by the tested compounds, which had an inhibition zone ranging from 15 to 33 mm, and in the case of fungal species an inhibition zone ranging from 13 to 32 mm was observed. The synthesized compound showed stronger and moderate action compared to reference medicines. The tested compound's antimicrobial activity was determined using a 100 μg/ml attentiveness of a molecule in the solvent DMSO. Figures 3 and 4 provide a graphical representation of the antimicrobial activity data.[42]

## Protocol of molecular docking study

The ChemSketch 2021.2.0 software was used for the generation of ligand structures. Furthermore, the docking studies were carried out to find the interacting residues of all compounds AutoDock Vina 1.1.2 was used and during the docking study the energy minimization of every molecule was performed using Avogadro-1.2.0.[43] The crystal structure of the 24 kDa domain of *E. coli* DNA gyrase was downloaded from the PDB data bank (4DUH). The structural receptor was devoid of all ligands before docking by excluding heteroatoms. Kollaman charge, solvation parameters, and polar hydrogens were added to the protein to complete its processing. For *x*, *y*, and *z*, the appropriate grid box sizes were set to 40, 40, and 40 Å. For each of the variables *x*, *y*, and *z*, the grid center was set to 29.712, 2.093, and 23.925. The exhaustiveness was 40 and the grid point spacing was 0.375 Å. The most likely binding mechanism was determined using the robust molecular graphics viewer Discovery Studio Visualizer v21.0.[44]

## Protocol of molecular dynamic simulation

The DESMOND module (Schrodinger Inc., USA) was used to conduct a molecular dynamics investigation on the best dock protein-ligand combination. The study was conducted using the Berendsen thermostat and barostat procedures for 100 ns. The system was solved, minimized, and put into a TIP3P orthorhombic box measuring $10 \times 10 \times 10$ Å. Desmond's Protein Preparation, Ligand Preparation, and Epik tools confirmed the chemical structure's precision. The minimized explicit solvation complex of the ligand-receptor complex was simulated for 100 ns using the NPT ensemble (at 300 K and 1.01325 bars). Steepest Descent and Broyden-Fletcher-Goldfarb-Shanno algorithms were used to relax the system. The dynamics simulation approach used the Nose-Hoover thermostat algorithm and the Martyna-Tobias-Klein barostat algorithm at 300 K temperature and 1 atm pressure and OPLS_2005 force field. To mimic physiological conditions counterions and 0.15 M sodium chloride were introduced to neutralize the models. The models underwent relaxation before stimulation and trajectories were stored for inspections at intervals of 100 ps and frames selected from MD trajectories at intervals of 100 ns post completions of the MDS run. The smooth particle mesh Ewald technique was used to manage both long-range and short-range coulombic interactions, with

endpoint values of 9.0 Å. MD simulations were run for 100 ns, and trajectory information was acquired in the remaining 2.0 ns. It is a classical technique used to efficiently calculate long-range coulombic interactions by splitting the interaction into short-range (real space) and long-range (reciprocal space) components. The real-space component is computed directly, while the reciprocal space component is computed using Fourier transforms. This method is highly accurate for calculating columbic interactions. The stability of the docked complexes, **4DUH-6j** was assessed by monitoring, root mean square deviation (RMSD), and root mean square fluctuations (RMSF).[45]

## Conclusion

A novel series of hybrid molecules of quinoline derivatives containing substituted isoxazole was synthesized and characterized using NMR, and Mass spectral analysis. All the synthesized molecules were evaluated for their antibacterial and antifungal properties. Most of the newly synthesized compounds showed excellent antibacterial efficacy against both pathogens. Out of all the synthesized compounds, two compounds **6j** and **6l** showed promising results in antimicrobial activity with the highest docking score of −8.3 and −7.9 kJ/mol. While compounds **6d–e**, and **6h–i** were able to show good or moderate antibacterial and antifungal activity. Furthermore, docking and MD analysis revealed that compound **6j** may have exhibited antimicrobial potency through inhibition of *E. coli* DNA gyrase.

## Disclosure statement

No potential conflict of interest was reported by the author(s).

## Funding

## ORCID

Satishkumar D. Tala 🔟 http://orcid.org/0000-0003-2151-3940

## References

[1] Weinstein, R. A.; Gaynes, R.; Edwards, J. R, National Nosocomial Infections Surveillance System. National Nosocomial Infections Surveillance System. Overview of Nosocomial Infections Caused by Gram-Negative Bacilli. *Clin. Infect. Dis.* **2005**, *41*, 848–854. DOI: 10.1086/432803.

[2] Penchovsky, R.; Traykovska, M. Designing Drugs That Overcome Antibacterial Resistance: Where Do We Stand and What Should We Do? *Expert Opin. Drug Discov.* **2015**, *10*, 631–650. DOI: 10.1517/17460441.2015.1048219.

[3] Nathan, C.; Cars, O. Antibiotic Resistance – Problems, Progress, and Prospects. *New Engl. J. Med.* **2014**, *371*, 1761–1763. DOI: 10.1056/NEJMp1408040.

[4]   Antimicrobial-Resistance. https://www.who.int/news-room/factsheets/detail/antimicrobial-resistance (accessed Nov, 2023).

[5]   *Antimicrobial Resistance: Global Report on Surveillance*; World Health Organization, **2023**. https://www.who.int/drugresistance/documents/surveillance%20report/en/.

[6]   Zhang, G. F.; Zhang, S.; Pan, B.; Liu, X.; Feng, L. S. 4-Quinolone Derivatives and Their Activities Against Gram Positive Pathogens. *Eur. J. Med. Chem.* **2018**, *143*, 710–723. DOI: 10.1016/j.ejmech.2017.11.082.

[7]   Troïa, T.; Siad, J.; Di Giorgio, C.; Brunel, J. M. Design and Synthesis of New Polyamine Quinoline Antibiotic Enhancers to Fight Resistant Gram-Negative *P. aeruginosa* Bacteria. *Eur. J. Med. Chem. Rep.* **2022**, *5*, 100054. DOI: 10.1016/j.ejmcr.2022.100054.

[8]   Tay, S. B.; Yew, W. S. Development of Quorum-Based Anti-Virulence Therapeutics Targeting Gram-Negative Bacterial Pathogens. *Int. J. Mol. Sci.* **2013**, *14*, 16570–16599. DOI: 10.3390/ijms140816570.

[9]   Mandewale, M. C.; Patil, U. C.; Shedge, S. V.; Dappadwad, U. R.; Yamgar, R. S. A Review on Quinoline Hydrazone Derivatives as a New Class of Potent Antitubercular and Anticancer Agents. *Beni-Suef Univ. J. Basic Appl. Sci.* **2017**, *6*, 354–361. DOI: 10.1016/j.bjbas.2017.07.005.

[10]  Abdi, B.; Fekadu, M.; Zeleke, D.; Eswaramoorthy, R.; Melaku, Y. Synthesis and Evaluation of the Antibacterial and Antioxidant Activities of Some Novel Chloroquinoline Analogs. *J. Chem.* **2021**, *2021*, 1–13. DOI: 10.1155/2021/2408006.

[11]  Kumar Gupta, S.; Mishra, A. Synthesis, Characterization and Screening for Anti-Inflammatory and Analgesic Activity of Quinoline Derivatives Bearing Azetidinones Scaffolds. *Antiinflamm. Antiallergy Agents Med. Chem.* **2016**, *15*, 31–43. DOI: 10.2174/1871523015666160210124545.

[12]  Goda, F. E.; Alaa, A. M.; Ghoneim, H. A. Synthesis and Biological Evaluation of Novel 6-Nitro-5-Substituted Aminoquinolines as Local Anaesthetic and Anti-Arrhythmic Agents: Molecular Modeling Study. *Bioorg. Med. Chem.* **2005**, *13*, 3175–3183. DOI: 10.1016/j.bmc.2005.02.050.

[13]  Jin, H. G.; Sun, X. Y.; Chai, K. Y.; Piao, H. R.; Quan, Z. S. Anticonvulsant and Toxicity Evaluation of Some 7-Alkoxy-4,5-Dihydro-[1,2,4]Triazolo[4,3-*a*]Quinoline-1(2*H*)-Ones. *Bioorg. Med. Chem.* **2006**, *14*, 6868–6873. DOI: 10.1016/j.bmc.2006.06.044.

[14]  Zajdel, P.; Marciniec, K.; Maślankiewicz, A.; Grychowska, K.; Satała, G.; Duszyńska, B.; Lenda, T.; Siwek, A.; Nowak, G.; Partyka, A.; et al. Antidepressant and Antipsychotic Activity of New Quinoline and Isoquinoline-Sulfonamide Analogs of Aripiprazole Targeting Serotonin 5-HT1A/5-HT2A/5-HT7 and Dopamine D2/D3 Receptors. *Eur. J. Med. Chem.* **2013**, *60*, 42–50. DOI: 10.1016/j.ejmech.2012.11.042.

[15]  Kumar, H.; Devaraji, V.; Joshi, R.; Jadhao, M.; Ahirkar, P.; Prasath, R.; Bhavana, P.; Ghosh, S. K. Antihypertensive Activity of a Quinoline Appended Chalcone Derivative and Its Site Specific Binding Interaction with a Relevant Target Carrier Protein. *RSC Adv.* **2015**, *5*, 65496–65513. DOI: 10.1039/C5RA08778C.

[16]  Muruganantham, N.; Sivakumar, R.; Anbalagan, N.; Gunasekaran, V.; Leonard, J. T. Synthesis, Anticonvulsant and Antihypertensive Activities of 8-Substituted Quinoline Derivatives. *Biol. Pharm. Bull.* **2004**, *27*, 1683–1687. DOI: 10.1248/bpb.27.1683.

[17]  Deshmukh, A. R.; Dhumal, S. T.; Nawale, L. U.; Khedkar, V. M.; Sarkar, D.; Mane, R. A. Dicationic Liquid Mediated Synthesis of Tetrazoloquinolinyl Methoxy Phenyl 4-Thiazolidinones and Their Antibacterial and Antitubercular Evaluation. *Synth. Commun.* **2019**, *49*, 587–601. DOI: 10.1080/00397911.2018.1564928.

[18]  Senerovic, L.; Opsenica, D.; Moric, I.; Aleksic, I.; Spasić, M.; Vasiljevic, B. Quinolines and Quinolones as Antibacterial, Antifungal, Anti-Virulence, Antiviral and Anti-Parasitic Agents. *Adv. Exp. Med. Biol.* **2020**, *1282*, 37–69. DOI: 10.1007/5584_2019_428.

[19]  Rodríguez, A. D.; Ramírez, C.; Rodríguez, I. I.; González, E. Novel Antimycobacterial Benzoxazole Alkaloids, from The West Indian Sea Whip Pseudopterogorgia Elisabethae. *Org. Lett.* **1999**, *1*, 527–530. DOI: 10.1021/ol9907116.

[20]  Mckee, M. L.; Kerwin, S. M. Synthesis, Metal Ion Binding, and Biological Evaluation of New Anticancer 2-(2′-Hydroxyphenyl)Benzoxazole Analogs of UK-1. *Bioorg. Med. Chem.* **2008**, *16*, 1775–1783. DOI: 10.1016/j.bmc.2007.11.019.

[21] Shaik, A.; Bhandare, R. R.; Palleapati, K.; Nissankararao, S.; Kancharlapalli, V.; Shaik, S. Antimicrobial, Antioxidant, and Anticancer Activities of Some Novel Isoxazole Ring Containing Chalcone and Dihydropyrazole Derivatives. *Molecules* **2020**, *25*, 1047. DOI: 10.3390/molecules25051047.

[22] Zhang, H. Z.; Zhao, Z. L.; Zhou, C. H. Recent Advance in Oxazole-Based Medicinal Chemistry. *Eur. J. Med. Chem.* **2018**, *144*, 444–492. DOI: 10.1016/j.ejmech.2017.12.044.

[23] Stokes, N. R.; Baker, N.; Bennett, J. M.; Chauhan, P. K.; Collins, I.; Davies, D. T.; Gavade, M.; Kumar, D.; Lancett, P.; Macdonald, R.; et al. Design, Synthesis and Structure – Activity Relationships of Substituted Oxazole–Benzamide Antibacterial Inhibitors of Ftsz. *Bioorg. Med. Chem. Lett.* **2014**, *24*, 353–359. DOI: 10.1016/j.bmcl.2013.11.002.

[24] Yamamuro, D.; Uchida, R.; Ohtawa, M.; Arima, S.; Futamura, Y.; Katane, M.; Homma, H.; Nagamitsu, T.; Osada, H.; Tomoda, H. Synthesis and Biological Activity of 5-(4-Methoxyphenyl) Oxazole Derivatives. *Bioorg. Med. Chem. Lett.* **2015**, *25*, 313–316. DOI: 10.1016/j.bmcl.2014.11.042.

[25] Zhong, Z.-J.; Zhang, D.-J.; Peng, Z.-G.; Li, Y.-H.; Shan, G.-Z.; Zuo, L.-M.; Wu, L.-T.; Li, S.-Y.; Gao, R.-M.; Li, Z.-R. Synthesis and Antiviral Activity of a Novel Class of (5-Oxazolyl) Phenyl Amines. *Eur. J. Med. Chem.* **2013**, *69*, 32–43. DOI: 10.1016/j.ejmech.2013.07.053.

[26] Palleapati, K.; Kancharlapalli, V. R.; Shaik, A. B. Synthesis, Characterization and Antitubercular Evaluation of Some New Isoxazole Appended 1-Carboxamido-4,5-Dihydro-1*H*-Pyrazoles. *J. Res. Pharm.* **2019**, *23*, 156–163. DOI: 10.12991/jrp.2019.120.

[27] Lee, H. K.; Yun, E.; Min, J. H.; Yoon, K. S.; Choung, D. H.; Lee, S. Convenient Synthesis of An Isoxazole Compound, KRIBB3, as An Anticancer Agent. *Synth. Commun.* **2012**, *42*, 1890–1894. DOI: 10.1080/00397911.2010.546551.

[28] Shakya, A. K.; Kaur, A.; Al-Najjar, B. O.; Naik, R. R. Molecular Modeling, Synthesis, Characterization and Pharmacological Evaluation of Benzo[*d*]Oxazole Derivatives as Non-steroidal Anti-Inflammatory Agents. *Saudi Pharm. J.* **2016**, *24*, 616–624. DOI: 10.1016/j.jsps.2015.03.018.

[29] Fonseca-Berzal, C.; Merchán Arenas, D. R.; Romero Bohórquez, A. R.; Escario, J. A.; Kouznetsov, V. V.; Gómez-Barrio, A. Selective Activity of 2,4-Diaryl-1,2,3,4-Tetrahydroquinolines on *Trypanosoma cruzi* Epimastigotes and Amastigotes Expressing B-Galactosidase. *Bioorg. Med. Chem. Lett.* **2013**, *23*, 4851–4856. DOI: 10.1016/j.bmcl.2013.06.079.

[30] Álvarez Santos, M. R.; Bueno Duarte, Y.; Güiza, F. M.; Romero Bohórquez, A. R.; Mendez-Sanchez, S. C. Effects of New Tetrahydroquinoline-Isoxazole Hybrids on Bioenergetics of Hepatocarcinoma HEP-G2 Cells and Rat Liver Mitochondria. *Chem. Biol. Interact.* **2019**, *302*, 164–171. DOI: 10.1016/j.cbi.2019.02.002.

[31] Bokkala, K.; Bapuram, A. K.; Thirukovela, N. S.; Nukala, S. K. Synthesis of Fused Isoxazoles of Iodoquinol as *In Vitro* EGFR Aiming Anticancer Agents. *ChemistrySelect* **2024**, *9*, e202302584. DOI: 10.1002/slct.202302584.

[32] Galenko, E. E.; Novikov, M. S.; Bunev, A. S.; Khlebnikov, A. F. Acridine–Isoxazole and Acridine–Azirine Hybrids: Synthesis, Photochemical Transformations in the UV/Visible Radiation Boundary Region, and Anticancer Activity. *Molecules* **2024**, *29*, 1538. DOI: 10.3390/molecules29071538.

[33] Güiza, F. M.; Duarte, Y. B.; Mendez-Sanchez, S. C.; Bohórquez, A. R. R. Synthesis and *In Vitro* Evaluation of Substituted Tetrahydroquinoline-Isoxazole Hybrids as Anticancer Agents. *Med. Chem. Res.* **2019**, *28*, 1182–1196. DOI: 10.1007/s00044-019-02363-z.

[34] Akbari, J. D.; Tala, S. D.; Dhaduk, M. F.; Joshi, H. S.; Mehta, K. B.; Pathak, S. J. Synthesis of Some New Pyrazolo[3,4-*d*]Pyrimidines and Thiazolo[4,5-*d*]Pyrimidines and Evaluation of Their Antimicrobial Activities. *Phosphorus Sulfur Silicon Relat. Elem.* **2008**, *183*, 1471–1477. DOI: 10.1080/10426500701681581.

[35] Thaker, K. M.; Ghetiya, R. M.; Tala, S. D.; Dodiya, B. L.; Joshi, K. A.; Dubal, K. L.; Joshi, H. S. Synthesis of Oxadiazoles and Pyrazolones as a Antimycobacterial and Antimicrobial Agents. *IJC-B* **2011**, *50B*, 738–744. doi:http://nopr.niscpr.res.in/handle/123456789/11693.

[36] Baruah, B.; Bhuyan, P. J. Synthesis of Some Complex Pyrano[2,3-*b*] and Pyrido[2,3-*b*] Quinolines from Simple Acetanilids via Intramolecular Domino Hetero Diels–Alder

Reactions of 1-Oxa-1,3-Butadienes in Aqueous Medium. *Tetrahedron* **2009**, *65*, 7099–7104. DOI: 10.1016/j.tet.2009.06.036.

[37] Bindu, P. J.; Mahadevan, K. M.; Satyanarayan, N. D.; Ravikumar Naik, T. R. Synthesis and DNA Cleavage Studies of Novel Quinoline Oxime Esters. *Bioorg. Med. Chem. Lett.* **2012**, *22*, 898–900. DOI: 10.1016/j.bmcl.2011.12.037.

[38] Steeneck, C.; Kinzel, O.; Anderhub, S.; Hornberger, M.; Pinto, S.; Morschhaeuser, B.; Braun, F.; Kleymann, G.; Hoffmann, T. Discovery of Hydroxyamidine Based Inhibitors of IDO1 For Cancer Immunotherapy With Reduced Potential for Glucuronidation. *ACS Med. Chem. Lett.* **2020**, *11*, 179–187. DOI: 10.1021/acsmedchemlett.9b00572.

[39] Aleti, R. R.; Cherukupalli, S.; Dhawan, S.; Kumar, V.; Girase, P. S.; Mohite, S.; Karpoormath, R. A. Metal-Free Approach for *In Situ* Regioselective Synthesis of Isoxazoles via 1,3-Dipolar Cycloaddition Reaction of Nitrile Oxide with Propargyl Bromide. *Chem. Pap.* **2022**, *76*, 3005–3010. DOI: 10.1007/s11696-021-02009-8.

[40] Ghannam, I. A.; Abd El-Meguid, E. A.; Ali, I. H.; Sheir, D. H.; El Kerdawy, A. M. Novel 2-Arylbenzothiazole DNA Gyrase Inhibitors: Synthesis, Antimicrobial Evaluation, QSAR and Molecular Docking Studies. *Bioorg. Chem.* **2019**, *93*, 103373. DOI: 10.1016/j.bioorg.2019.103373.

[41] Childers, M. C.; Daggett, V. Insights from Molecular Dynamics Simulations for Computational Protein Design. *Mol. Syst. Des. Eng.* **2017**, *2*, 9–33. DOI: 10.1039/C6ME00083E.

[42] Bakht, J.; Khan, S.; Shafi, M. *In Vitro* Antimicrobial Activity of *Allium cepa* (Dry Bulbs) Against Gram Positive and Gram-Negative Bacteria and Fungi. *Pak. J. Pharm. Sci.* **2014**, *27*, 139–145. DOI: 10.1016/j.micpath.2018.08.008.

[43] Trott, O.; Olson, A. J. Software News and Update Autodock Vina: Improving the Speed and Accuracy of Docking with a New Scoring Function. *J. Comput. Chem.* **2009**, *31*, 455–461. DOI: 10.1002/jcc.21334.

[44] Dassault Systemes Biovia. *Discovery Studio Modeling Environment, Release 2017*; Dassault Systemes: San Diego, CA, **2017**.

[45] De Souza, O. N.; Ornstein, R. L. Effect of Warmup Protocol and Sampling Time on Convergence of Molecular Dynamics Simulations of a DNA Dodecamer Using AMBER 4.1 and Particle-Mesh Ewald Method. *J. Biomol. Struct. Dyn.* **1997**, *14*, 607–611. DOI: 10.1080/07391102.1997.10508160.